JOC Article
pubs.acs.org/joc

New Insight into Chiroptical Properties of 1,2-Diols Cyclic Sulfites.

Paweł Chochrek,[†] Jadwiga Frelek,*[,†] Marcin Kwit,[‡] and Jerzy Wicha[†]

[†]*Institute of Organic Chemistry of the Polish Academy of Sciences, Kasprzaka 44, 01-224 Warsaw, Poland, and* [‡]*Faculty of Chemistry, Adam Mickiewicz University, Grunwaldzka 6, 60-780 Poznań, Poland*

frelek@icho.edu.pl

Received June 22, 2009

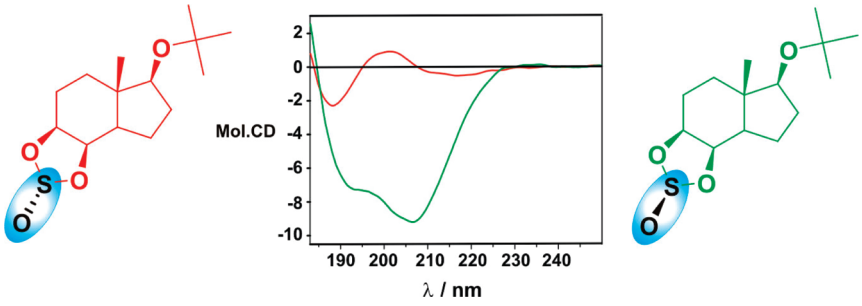

The present work examines the relationship between the structure and chiroptical properties of cyclic sulfites utilizing the electronic circular dichroism (CD) and time-dependent density functional theory (TD-DFT). For some of the model compounds the study was additionally supported by the X-ray diffraction analysis. A comparison of the experimental and simulated CD spectra gave a reasonable interpretation of the Cotton effects observed in the 200−220 nm spectral range. The study revealed a high sensitivity of the CD spectra with regard to the configuration at the sulfur atom as well as the conformation of the ring bearing the sulfite chromophore. The results demonstrated that such a combined treatment enabled the determination of absolute configuration with a high degree of confidence.

Introduction

Cyclic sulfites are conveniently prepared by the reaction of 1,2- or 1,3-diols with thionyl chloride or with its synthetic equivalents, such as sulfur tetrachloride (followed by hydrolysis) or dimethyl sulfite.[1] The sulfur atom is stereogenic in cyclic sulfites derived from the chiral diols. This results in the existence of two sulfur-centered epimers. Surprisingly, little attention has been devoted to the stereochemical aspects of cyclic sulfites related to natural products.[2] Only recently, Garcia-Grandos and co-workers[3] have reported preparation and biotransformations of diastereomeric pairs of sesquiterpene-related cyclic sulfites. Single-crystal X-ray analysis has been employed to determine the absolute configuration (AC) at the sulfur atom in the diastereomers. Since these cyclic sulfites show absorption maximum in the UV spectral range at around 195−220 nm,[4] it could be expected that an important stereochemical information could be gained from their electronic circular dichroism (CD) spectra. Indeed, Sarel and co-workers[4] have shown that the CD spectra of model cyclic sulfites derived from chiral 1,2-diols reflect the configuration at the sulfur atom. More recently, our study on application of the CD in determination of the AC of six-membered cyclic sulfites derived from glucofuranose and 1,2,4-butanetriol revealed the usefulness of CD spectroscopy for this purpose.[5] In view of growing interest in the synthesis and applications of chiral 1,2-diols,[6] it became important to acquire a new insight into chiroptical properties of 1,2-diol cyclic sulfites. Owing to the high sensitivity and accessibility of CD spectroscopy, its

(1) Byun, H. S.; He, L. L.; Bittman, R. *Tetrahedron* **2000**, *56*, 7051–7091. Lohray, B. B. *Synthesis* **1992**, 1035–1052. van Woerden, H. F. *Chem. Rev.* **1963**, *63*, 557–571.
(2) Herzig, P. T.; Ehrenstein, M. *J. Org. Chem.* **1952**, *17*, 724–736.
(3) Garcia-Granados, A.; Parra, A.; Rivas, F.; Segovia, A. J. *J. Org. Chem.* **2007**, *72*, 643–646. Garcia-Granados, A.; Gutierrez, M. C.; Rivas, F. *Org. Biomol. Chem.* **2003**, *1*, 2314–2320.
(4) Usieli, V.; Pilersdorf, A.; Shor, S.; Katzhendler, J.; Sarel, S. *J. Org. Chem.* **1974**, *39*, 2073–2079.
(5) Borsuk, K.; Frelek, J.; Łysek, R.; Urbańczyk-Lipkowska, Z.; Chmielewski, M. *Chirality* **2001**, *13*, 533–540.
(6) Kolb, H. C.; VanNieuwenhze, M. S.; Sharpless, K. B. *Chem. Rev.* **1994**, *94*, 2483–2547. Caron, P.; Dugger, R. W.; Ruggeri, S. G.; Ragan, J. A.; Ripin, D. H. B. *Chem. Rev.* **2006**, *106*, 2943–2989.

Published on Web 08/28/2009 DOI: 10.1021/jo9012964

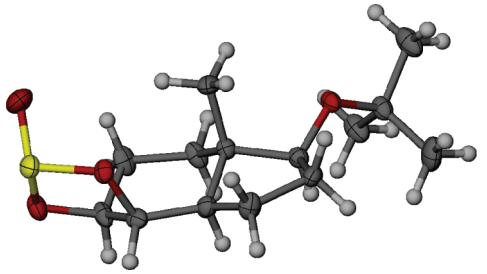

FIGURE 1. ORTEP diagram of X-ray structure of compound **5b**. Thermal ellipsoids are shown at 50% probability level.

CHART 1

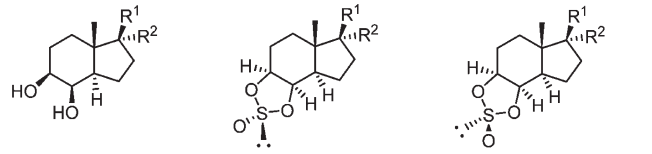

1, R^1 = O^{t}Bu, R^2 = H
2, R^1 and R^2 = O
3, R^1 = C_8H_{17}, R^2 = H
4, $R^1$and R^2 = CHMe (*Z*)

5a, R^1 = O^{t}Bu, R^2 = H
6a, R^1 = OH, R^2 = H
7a, R^1 = C_8H_{17}, R^2 = H
8a, $R^1$and R^2 = CHMe (*Z*)

5b, R^1 = O^{t}Bu, R^2 = H
6b, R^1 = OH, R^2 = H
7b, R^1 = C_8H_{17}, R^2 = H
8b, $R^1$and R^2 = CHMe (*Z*)

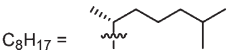

application to cyclic sulfites, combined with the theoretical calculation using density functional theory (DFT), may result in establishing a convenient and reliable method to assign the AC at the sulfur atom. To the best of our knowledge, there are no prior DFT reports on the optical activity of sulfites. Therefore, we decided to undertake a detailed study on this subject in order to examine the reliability of the CD method and to establish its scope and limitations. Moreover, we decided to support our experimental and theoretical chiroptical studies by the X-ray data, where possible.

Results and Discussion

The diols **1**−**4** (Chart 1) have been chosen for the studies. The diol **1** has been prepared in one of our laboratories in conjunction with the synthesis of certain vitamin D analogues.[7] The reaction of diol **1** with thionyl chloride in dichloromethane, in the presence of pyridine (0 °C to rt), afforded a mixture of sulfites **5a** (S_R) and **5b** (S_S) that were resolved by chromatography. The X-ray structures for both diastereomers were obtained. The ORTEP plot of the structure of **5b** is presented in Figure 1 (for the X-ray structure of the isomer **5a**, see ref 7).

Since the theoretical calculations have also been planned, simpler model compounds lacking the *tert*-butyl group, **6a** and **6b**, were also needed. All our attempts to hydrolyze selectively the *tert*-butyl ether in a mixture of **5a** and **5b** failed. Eventually, these compounds were synthesized from the respective diacetate **9**[7] as indicated in Scheme 1. Treatment of **9** with cerium(III) chloride heptahydrate and sodium iodide, in acrylonitrile, according to the procedure of Bartoli et al.[8] smoothly cleaved the *tert*-butyl ether linkage to afford **10** in 97% yield. The hydroxy group in **10** was then oxidized with PCC, and diacetoxy ketone **11** was hydrolyzed to give diol **2**. The latter was reacted with thionyl chloride under standard conditions to afford a mixture of unstable cyclic sulfinates. The mixture was treated with sodium borohydride in ethanol to stereoselectively reduce the carbonyl group to a 1β-hydroxy group. Finally, the isomers differing in the configuration at the sulfur atom, **6a** and **6b**, were separated using preparative HPLC (a ratio of **6a**:**6b** as 71:29).

Diols **3** and **4** were reported previously.[9] Their reaction with thionyl chloride afforded the mixture of the respective sulfites.

The ratios of isolated isomeric cyclic sulfites are as follows: **5a**:**5b**, 76:23;[7] **6a**:**6b**, 71:29; **7a**:**7b**, 73:27; and **8a**:**8b**, 81:19.

Chiroptical Spectra. The electronic absorption and chiroptical data of sulfites **5a**−**8b** are collected in Table 1. As an example, the CD spectra of sulfite **5b** recorded both in solution and in the solid state are presented in Figure 2.

As can be seen in Table 1, the electronic absorption spectra of sulfites **5a**−**8b** show only one maximum of moderate intensity at around 198 nm. Similarly to the six-membered sulfites described previously,[5] the CD data of sulfites in question demonstrate that the investigated compounds fall under two distinct classes with respect to the number of Cotton effects (CEs) in their CD spectra and the intensity of the CD band occurring at around 200 nm (Table 1). Compounds from the first class (class "**a**"), consisting of sulfites **5a**, **6a**, **7a**, and **8a**, show three CD bands of moderate intensity at around 215, 200, and 185 nm. Sulfites **5b**, **6b**, **7b**, and **8b**, which form the second class (class "**b**"), are characterized by two negative CD bands of considerable intensity located at around 200 and 187 nm (Figure 2).

The X-ray data of sulfites **5a**[7] and **5b** (Figure 2), the only two compounds among the investigated group which form suitable crystals for X-ray analysis, allowed us to establish the AC to be $S_{(R)}$ and $S_{(S)}$, respectively. For both of these compounds (**5a** and **5b**), with their structures and stereochemistry confirmed by X-ray analysis, the CD curves in the solid state were also measured. The obtained solid-state spectra are in very good agreement with the respective data recorded in solution (Figure 2 for **5b** and Supporting Information Figure A for **5a**), thus providing additional proof that the same molecular species are present in the solid state as well as in solution. The similarity of the spectra recorded in various solvents and in Nujol mull as well as in KCl pellet indicates that the solute−solvent interactions, which may considerably affect the CD spectra due to conformational and vicinal effects, are negligible in this case and points out that the observed CD is largely a molecular property. Therefore, the analysis of the CD data for the purpose of determination of the AC of sulfites **5a**−**8b** can be performed on the basis of chiroptical data recorded for respective solutions.

On the basis of the known configuration of sulfites **5a** and **5b**, the absolute stereochemistry at the sulfur atom should be the same as for the remaining sulfites from the "**a**" and "**b**" class, respectively. Consequently, it can be unambiguously established that the AC at the sulfur atom in the "**a**" class of sulfites is $S_{(R)}$ while in the "**b**" class it is $S_{(S)}$.

(7) Chochrek, P.; Wicha, J. *J. Org. Chem.* **2007**, *72*, 5276–5284.
(8) Bartoli, G.; Bosco, M.; Locatelli, M.; Marcantoni, E.; Melchiorre, P.; Sambri, L. *Org. Lett.* **2005**, *7*, 427–430.
(9) Chochrek, P.; Kurek-Tyrlik, A.; Michalak, K.; Wicha, J. *Tetrahedron Lett.* **2006**, *47*, 6017–6020.

SCHEME 1

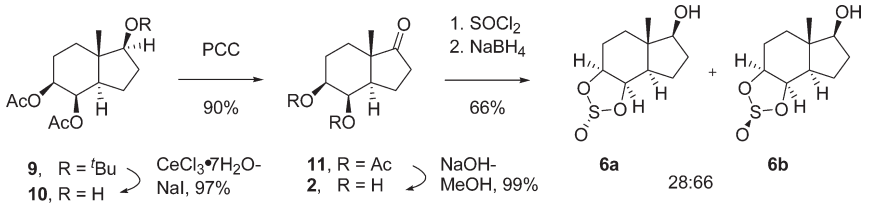

TABLE 1. UV and CD Data of Sulfites 5−8 Measured in Acetonitrile[a]

compd	UV ε (λ_{max}/nm)		CD $\Delta\varepsilon$ (λ_{max}/nm)	
5a	1780 (198);	−2.72 (188.5);	+1.73 (198.5);	−0.66 (215.5)
5b	1570 (203)	−6.09 (189.0);	−11.45 (203.8)	
6a	2600 (198);	−3.11 (186.0);	+0.63 (199.5);	−0.57 (214.5);
6b	3000 (203);	−6.50 (187.0)	−10.42 (204.0);	
7a	1710 (198);	−1.67 (184.5);	+1.41 (199.0);	−0.58 (215.5)
7b	2450 (200)	−3.61 (189.0);	−8.02 (204.0)	
8a	9500 (195);	−11.30 (187.5);	+1.83 (206.0);	−0.46 (219.0);
8b	8960 (197);	−12.66 (185.0)	−15.31 (202.0);	

[a]UV and CD values are given as ε (nm) and $\Delta\varepsilon$ (nm), respectively.

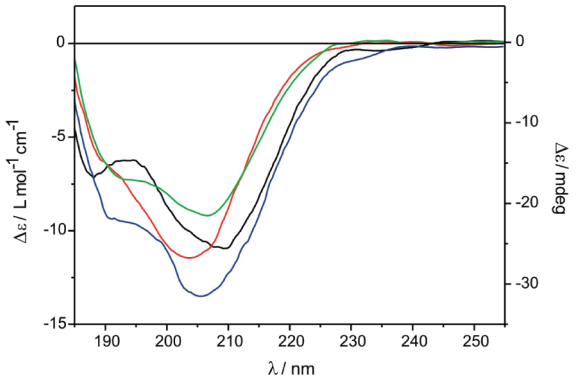

FIGURE 2. CD spectra of sulfite **5b** recorded in hexane (green line), acetonitrile (red line), KCl pellet (black line), and Nujol mull (blue line). Data recorded in Nujol is given in millidegrees.

Diastereomeric compounds from the "**a**" and "**b**" classes differ from each other by the S→O configuration only. Hence, one may conclude that the stereochemistry at sulfur atom (the first sphere, according to Snatzke[10]) is responsible for the sign pattern of the CD curves of sulfites **5a**−**8b**. However, the value of their dissymmetry factor g, equal to approximately 3×10^{-3}, is characteristic for molecules of class II according to Moscowitz, i.e., to those whose chromophore is locally achiral but is perturbed by its chiral surroundings.[11] Thus, the chiral sphere nearest to the chromophore mainly determines the sign and the magnitude of the Cotton effect. Therefore, the difference in substitution and conformation of the ring influences the CD significantly and for that reason the sterostructure of sulfites **5a**−**8b** was studied in minute detail, as presented in the following section.

Conformational Analysis. In an effort to corroborate the stereochemical conclusions made on the basis of the experimental data, the CD spectra of sulfites **5a**−**8b** were computed by applying the time-dependent density functional theory (TD-DFT). However, prior to the calculation of chiroptical properties of **5a**−**8b**, the conformational searches were carried out to evaluate the stable conformation of these compounds. The proper conformational analysis of target molecule is of critical importance, especially for the flexible compounds where the relative energies of participating conformers should be calculated with the highest available accuracy.[12] It has been shown that even a minor changes in the conformation of molecule can result in a change of sign and/or magnitude of calculated CD.[13]

CHART 2. Model Compounds Used for Calculation

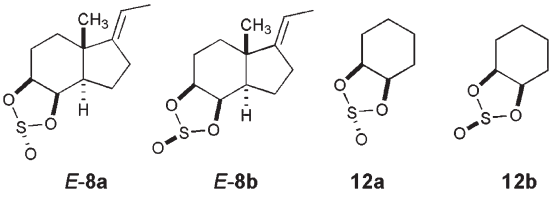

In the case of the conformational search of sulfites **7a** and **7b**, the long alkyl chain was replaced by the methyl group for simplification of calculation. Both methyl and octyl groups have the same electronic properties and do not influence electronic spectra. Additionally, we performed the computational analyses for *E*-isomers of **8a** and **8b** as well as for the model compounds **12a**,**b** (Chart 2).

The results of our DFT-B3LYP/6-311++G(2d,2p) calculations for **5a**−**8b** are presented in Table 2 and Figure 3.

(10) Snatzke, G. *Angew. Chem., Int. Ed.* **1979**, *18*, 363–377.
(11) Moscowitz, A. *Tetrahedron* **1961**, *13*, 48–56.

(12) Stephens, P. J.; McCann, D. M.; Butkus, E.; Stončius, S.; Cheeseman, J. R.; Frisch, M. J. *J. Org. Chem.* **2004**, *69*, 1948–1958. Stephens, P. J.; McCann, D. M.; Devlin, F. J.; Cheeseman, J. R.; Frisch, M. J. *J. Am. Chem. Soc.* **2004**, *126*, 7514–7521. Stephens, P. J.; McCann, D. M.; Devlin, F. J.; Smith, A. B., III. *J. Nat. Prod* **2006**, *69*, 1055–1064.
(13) Kundrat, M. D.; Autschbach, J. *J. Phys. Chem. A* **2006**, *110*, 4115–4123. Kundrat, M. D.; Autschbach, J. *J. Phys. Chem. A* **2006**, *110*, 12908–12917. Kwit, M.; Sharma, N. D.; Boyd, D. R.; Gawronski, J. *Chem.—Eur. J.* **2007**, *13*, 5812–5821. Kwit, M.; Sharma, N. D.; Boyd, D. R.; Gawronski, J. *Chirality* **2008**, *20*, 609–620. Marchesan, D.; Coriani, S.; Forzato, C.; Nitti, P.; Pitacco, G.; Ruud, K. *J. Phys. Chem. A* **2005**, *109*, 1449–1453. Pecul, M. *Chem. Phys. Lett.* **2006**, *418*, 1–10. Pecul, M.; Ruud, K.; Rizzo, A.; T, H. *J. Phys. Chem. A* **2004**, *108*, 4269–4276. Specht, K. M.; Nam, J.; Ho, D. M.; Berova, N.; Kondru, R. K.; Beratan, D. N.; Wipf, P.; Pascal, P. A., Jr.; Kahne, A. *J. Am. Chem. Soc.* **2001**, *123*, 8961–8966. Wiberg, K. B.; Vaccaro, P. H.; Cheeseman, J. R. *J. Am. Chem. Soc.* **2003**, *125*, 1888–1896.

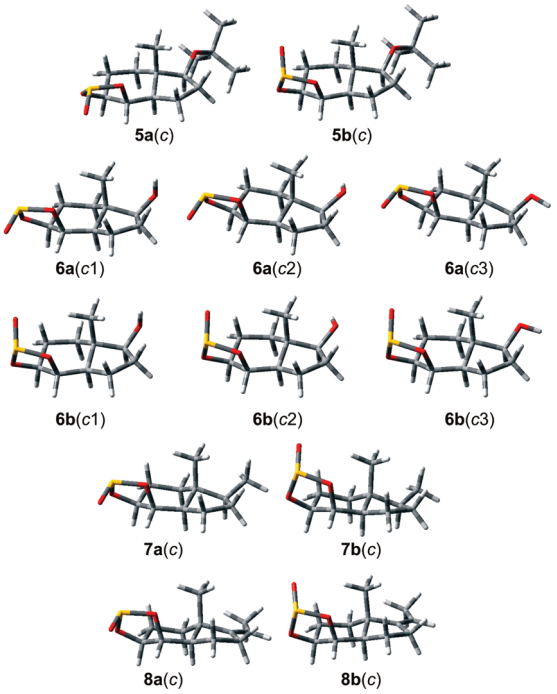

FIGURE 3. Structures of the low energy conformers of **5a**−**8b** calculated at B3LYP/6-311++G(2d,2p) theory level.

TABLE 2. Relative Energies (ΔE, ΔG) Calculated at the B3LYP/6-311++G(2d,2p) Level and Population Distribution of Stable Conformers of 5a−8b

conformer[a]	ΔE (kcal mol^{-1})	population (%)	ΔG (kcal mol^{-1})	population (%)
5a(*c*)	0.00	∼100	0.00	∼100
5a(*b*)	2.87		3.31	
5b(*c*)	0.00	∼100	0.00	∼100
5b(*b*)	6.02		5.82	
6a(*c*1)	0.00	41	0.00	36
6a(*c*2)	0.16	31	0.06	32
6a(*c*3)	0.24	28	0.06	32
6a(*b*1)	2.67		2.77	
6a(*b*2)	2.85		2.86	
6a(*b*3)	2.99		2.97	
6b(*c*1)	0.00	50	0.00	42
6b(*c*2)	0.31	29	0.13	33
6b(*c*3)	0.50	21	0.29	25
6b(*b*1)	5.70		5.00	
6b(*b*2)	6.40		5.61	
6b(*b*3)	6.18		5.43	
7a(*c*)	0.00	∼100	0.00	∼100
7a(*b*)	2.92		3.15	
7b(*c*)	0.00	∼100	0.00	∼100
7b(*b*)	6.00		5.46	
8a(*c*)	0.00	∼100	0.00	∼100
8a(*b*)	2.16		2.18	
8b(*c*)	0.00	∼100	0.00	∼100
8b(*b*)	5.28		5.95	

[a] *c* or *b* denotes chair or boat conformation of the six-membered ring.

The data for compounds **12a**,**b** is shown in the Supporting Information (Figures B and C, respectively).

As expected, for **5a**−**8b** a relatively small number of low-energy conformers have been found in the ΔE range between 0 and 2 kcal mol^{-1}. All structures belong to the same structural class characterized by the chair (*c*) conformation of the six-membered ring, regardless of the absolute configuration at the sulfur atom and the substitution pattern at C(1) (Figure 3).

For sulfites **5**−**7**, the five-membered ring adopts an envelope conformation, while for sulfites **8** the five-membered ring adopts a half-chair conformation due to the presence of an sp^2 carbon atom at position C(1). For sulfites **6a**,**b**, with a small hydroxyl substituent at the C(1) carbon atom, there are three conformers slightly differing in their relative energies. These conformers are generated by the rotation around the C(1)−O bond. However, in both **6a** and **6b** the *anti* conformation (in relation to the C(1)−H bond) of the hydroxy group is preferred. In the structurally similar sulfites **5a**,**b**, the bulky *tert*-butoxy substituent can only adopt the *syn* conformation relatively to the C(1)−H bond. Any deviation from this conformation causes the relative energy to increase, due to the steric repulsion between the *tert*-butyl and methyl and/or methylene groups. It is worth adding that the calculated geometry of **5b** is in excellent agreement with the one found in the solid state (see Figures 1 and 3)

In the second lowest energy conformers of sulfites **5a**−**8b**, the six-membered ring adopts a slightly twisted boat (*b*) conformation (see Figure B, Supporting Information) while the five-membered ring adopts an envelope or a twisted-envelope conformation depending on the type of substituent at C(1). As expected, the cyclohexyl ring inversion causes a significant increase of the relative energy. Since the relative energies of twisted boat (*b*) conformers are calculated as more then 2 kcal mol^{-1} higher compared to their respective low energy counterparts, only conformers of the *c*-type were taken into the further consideration.

Simulated UV and ECD Spectra. In order to correlate the observed chiroptical phenomena with the structures of investigated molecules, the CD spectra for all conformers of **5a**−**8b** in the framework of TD-DFT were calculated. The calculations were performed using the B3LYP hybrid functional in conjunction with the 6-311++G(2d,2p) and 6-311++G(2df,2p) basis sets. Although each experimental spectrum was reproduced acceptably by both the B3LYP/6-311++G(2d,2p) and B3LYP/6-311++G(2df,2p) methods, a better overall agreement was obtained at the B3LYP/6-311++G(2d,2p) level of theory; hence, we focus here only on the CD spectra calculated at the TD-B3LYP/6-311++G(2d,2p) level (see also the Supporting Information).[14] We also noted that the TD-B3LYP/6-311++G(2d,2p) consistently underestimated the excitation energy by ca. 5−15 nm, depending on the molecule.

The simulated CD spectra of sulfites with an *R* absolute configuration at the sulfur atom exhibit a negative CE at around 220 nm and a positive band at ca. 200 nm (Figure 4). The computed CD spectrum of **6a** is an exception since there is no positive CE at 200 nm, likely due to the underestimation of population of conformer **6a**(*c*1) in conformational equilibrium. The simulated spectrum for **8a** is slightly red-shifted in comparison to the measured one; however, the CD curve shape resembles other CD spectra of sulfites belonging to the same class. In general, the simulated CD spectra of sulfites with the $S_{(S)}$ configuration show only one negative CE at around 200 nm (Figure 4). Only in the case of the calculated spectrum of **5b** are there two negative CEs of approximately the same intensity at 195 and 210 nm.

(14) Trindle, C.; Altun, Z. *Theor. Chem. Acc.* **2009**, DOI 10.1007/s00214-008-0494-8.

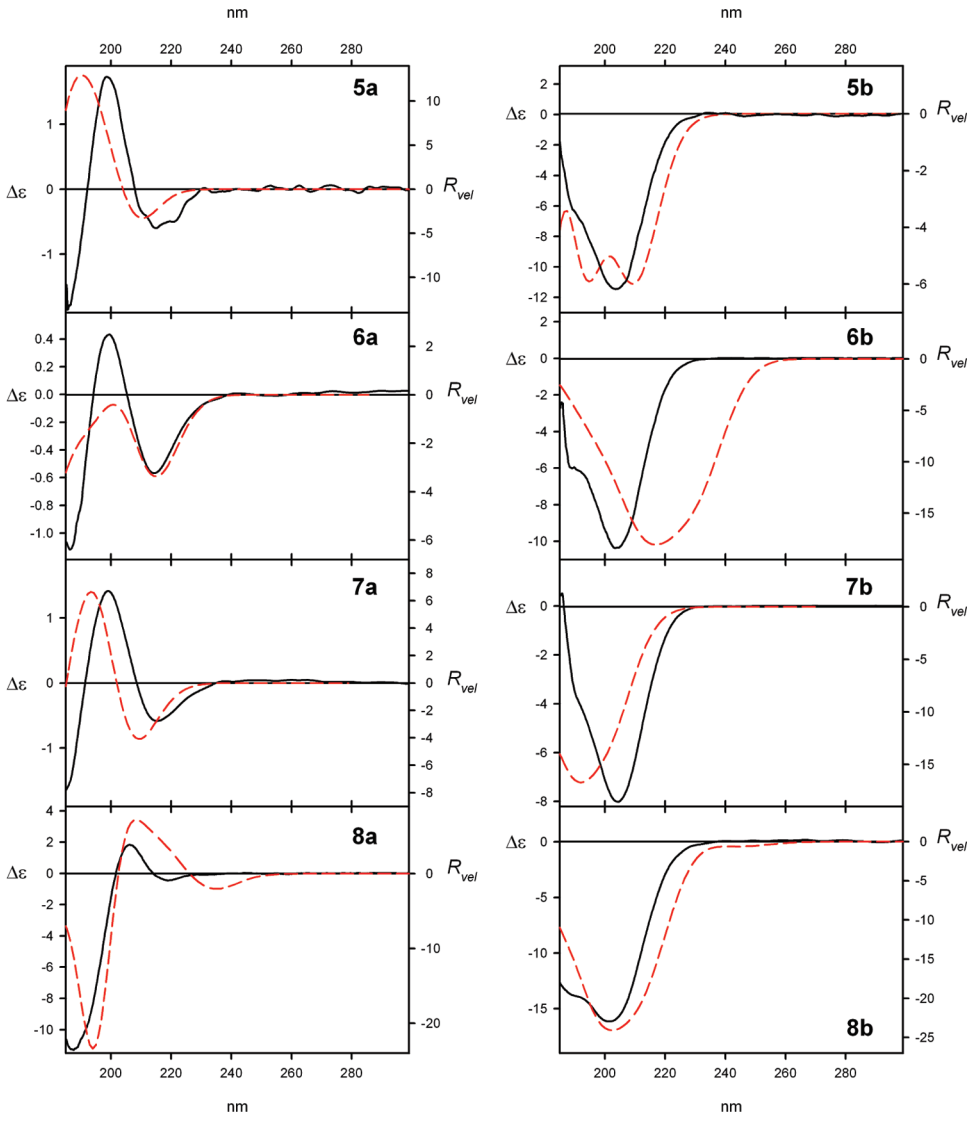

FIGURE 4. ECD spectra for sulfites **5a**−**8b**, experimental (solid black lines) and calculated at the TD-B3LYP/6-311++G(2d,2p) level (dashed red lines), averaged on the basis of the Boltzmann population. All calculated spectra are scaled in rotatory strength (R_{vel}) and are wavelength corrected to match the experimental UV spectra.

In order to clarify the origin of observed CEs, both the oscillator and rotatory strengths for chair and boat conformers of model compounds **12a** and **12b** were calculated by using the TD-B3LYP/6-311++G(2d,2p) level of theory (Figure 5 and Figure C in the Supporting Information). Structures of the model compounds were constructed from the optimized structures of the parent molecules by replacement of the five-membered ring with hydrogen atoms. These structures were not reoptimized and all possess trivial C_1 symmetry. The oscillator strengths appearing in the range of 250−200 nm are of almost the same moderate intensity for both conformers of **12a**. In the case of conformers of **12b**, the oscillator strengths differ in magnitudes −the electronic transitions calculated at around 220 nm are much more intense than those at around 200 nm. However, in all cases the origin of calculated excitations is the same. The 220 nm transition arises primarily from the HOMO−LUMO orbital excitation, whereas for the 200 nm one the major contribution is given by the excitation from the HOMO-1 to LUMO orbitals. This transition is mainly of the $n_{(O)}-\pi^*$ type, whereas the lowest energy transition at 220 nm is an admixture of mainly of $n_{(S)}-\pi^*$ and $n_{(O=S)}-\pi^*$ types (see Figure 5, right). In the case of **12a**, the rotatory strengths generated by these transitions have opposite sign but possess almost the same magnitude while for **12b**(*c*) they have the same sign and a similar magnitude. However, in the case of boat conformer of **12b** both excitations significantly differ in magnitude and are of opposite sign. Thus, the simulated ECD spectra for both conformers of **12a** are in a mirror image relationship. In the case of chair and boat conformers of **12b**, however, the simulated CD spectra have opposite sign for the long wavelength CE only. This is due to the dominating influence of negative rotatory strengths at 192 nm on the overall CD spectrum.

The results of our computation exercise demonstrated that the ring inversion dramatically affects the CD spectra, although the origin of calculated rotatory strengths remains the same. Nevertheless, the contribution of boat conformers

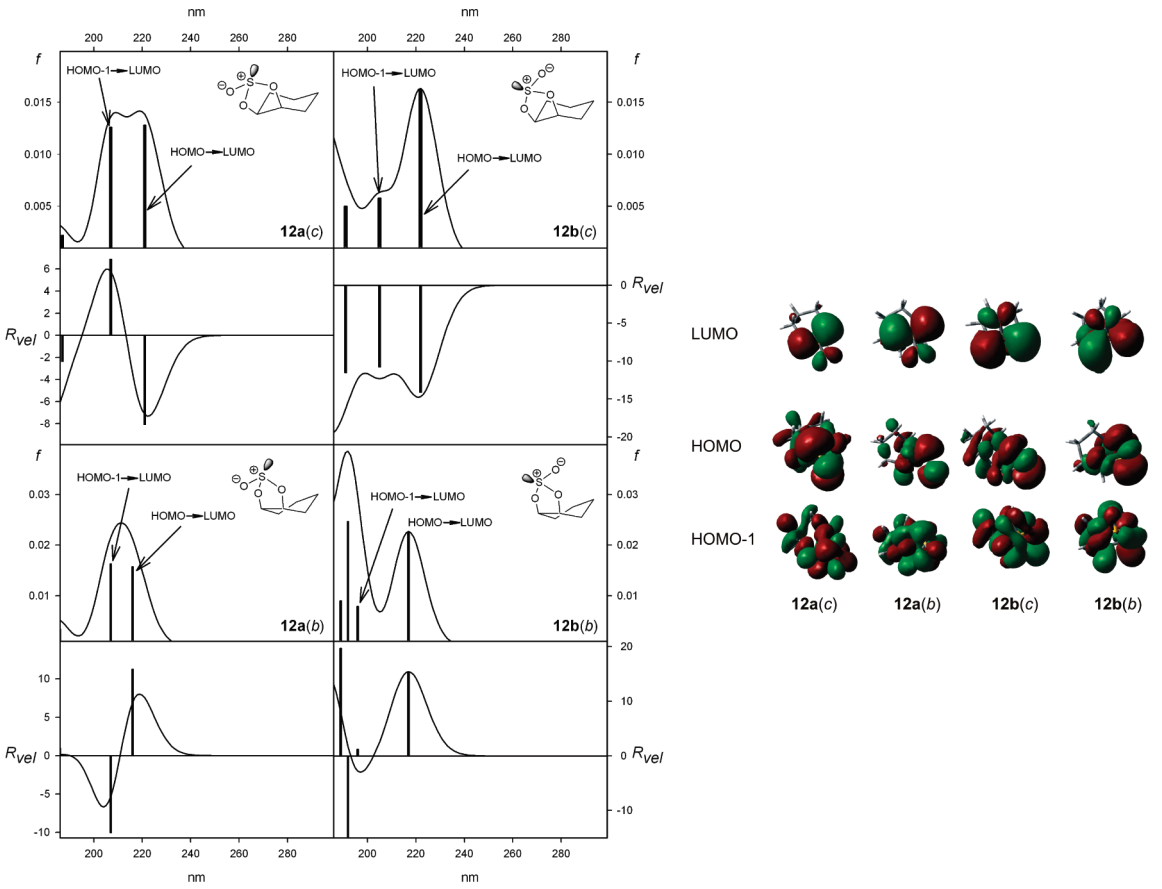

FIGURE 5. (Left) UV (upper panels) and CD (lower panels) spectra, calculated at the TD-B3LYP/6-311++G(2d,2p) level of theory, and oscillator and rotatory strengths (vertical bars) for model compounds **12a**(*c*), **12a**(*b*), **12b**(*c*), and **12b**(*b*). The calculated spectra were not wavelength corrected. (Right) Orbitals involved in low-energy electronic transitions in the case of model compounds **12a**(*c*), **12a**(*b*), **12b**(*c*), and **12b**(*b*).

to the net CD spectra of sulfites **5a**−**8b** is negligible due to their much higher energy.

The origin of CEs observed in sulfites **5a**−**7b** is the same as in model compounds **12a** and **12b**. Compounds **8a** and **8b** are the exception due to the presence of double bond in a chiral environment, which may strongly influence the CD spectra. In fact, the electronic transitions calculated for **8a**(*c*) at 241 nm and for **8b**(*c*) at 246 nm involve the HOMO−LUMO orbitals, and both possess $\pi-\pi^*$ character. The rotatory strengths generated by these electronic transitions are negative for both **8a**(*c*) and **8b**(*c*); however, this is clearly visible in experimental and simulated CD only in the case of compound **8a** (see Figure D in the Supporting Information). The electronic transitions that involve the n orbitals of oxygen and/or sulfur atoms appear at higher energies: the transitions of type $n_{(S)}-\pi^*$ and $n_{(O=S)}-\pi^*$ are calculated at 221 and 223 nm for **8a**(*c*) and **8b**(*c*), respectively, while the ones of $n_{(O)}-\pi^*$ type are calculated at 210 nm for **8a**(*c*) and at 208 nm for **8b**(*c*). The sign of rotatory strengths calculated at 221 and 210 nm for **8a**(*c*) is positive, whereas it is negative for rotatory strengths calculated at 223 and 208 nm for **8b**(*c*). It is worth adding that a general correlation between the *E* or *Z* configuration of double bond and the sign of observed and calculated long-wavelength CEs does not exist (see Figures D and E in the Supporting Information). The simulated CD and UV spectra for *E*-isomers of **8a** and **8b** show the positive sign of the long-wavelength CE for *E*-**8a**(*c*) (opposite to the one calculated for **8a**(*c*)), while in the case of both *E*-**8b**(*c*) and **8b**(*c*) the sign of the long wavelength CE is negative.

Conclusions

The relationship between the molecular structure and the chiroptical properties of sulfites **5**−**8** was investigated by means of the X-ray diffraction analysis, electronic circular dichroism spectroscopy, and the time-dependent density functional theory. To the best of our knowledge, such a combined treatment of the CD spectroscopy and theoretical calculation has been applied to study the chiral sulfites for the first time. The present report shows that the CD spectra of sulfites **5a**−**7b** depend strongly on the stereochemistry at sulfur atom and the conformation of cyclohexyl ring. Depending upon the $S_{(R)}$ or $S_{(S)}$ absolute configuration the spectra display three or two sufficiently developed CD bands, respectively. Furthermore, these bands differ in the magnitude of particular CEs which is stronger for the $S_{(S)}$ diastereomers. Thus, the differentiation between sulfur epimers in cyclic sulfites becomes readily available.

Additional but smaller dependence was found due to the type and conformation of substituent at C(1). In the case of sulfites **8a** and **8b**, the shape of their CD curves resembles the shape of CD spectra of **5a**−**7b**, respectively; however, the origin of CEs is different −for sulfites with the olefinic substituent at C(1) the sign of the long wavelength CE is

determined mainly by transitions involving π electrons of the double bond.

In general, the simulated spectra resemble smoothed experimental spectra and represent the theoretical and experimental estimates of rotational strength faithfully and equivalently. The very good agreement between the simulated and the experimental CD spectra allows one to assign the absolute configuration at sulfur atom in sulfites **5**−**8** with satisfactory accuracy. Recapitulating, CD spectroscopy was found to be a highly sensitive probe for the three-dimensional molecular structure around the sulfur atom in cyclic sulfites.

Experimental Section

The UV spectra were measured using a Cary 100 spectrophotometer in acetonitrile solutions. The CD spectra, recorded on a JASCO J-815 spectropolarimeter as mdeg spectra, were converted into $\Delta\varepsilon_{max}$ [L mol^{-1} cm^{-1}]/λ [nm] units. Solvents for circular dichroism measurements were spectroscopic grade. The solutions were examined between 185 and 300 nm at room temperature in cells with the path length of 0.05−1 cm and concentrations in the range of 0.8×10^{-4} to 1.2×10^{-3} mol·dm^{-3}. For the solid-state CD measurements, a crystalline compound (1−3 mg) and KCl (280−300 mg) or Nujol were ground and formed into a disk or a Nujol mull, which were rotated around the optical axis during the entire measurement. The solid-state CD measurements were performed using original JASCO equipment prepared for our instrument.

Preparation of New Model Compounds.

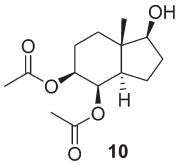

10

4,5-*O*,*O*-Diacetyl-(1*S*,3a*R*,4*R*,5*S*,7a*S*)-7a-methyloctahydro-1*H*-indene-1,4,5-triol (10). NaI (0.56 g, 3.75 mmol) and $CeCl_3 \times 7H_2O$ (1.40 g, 3.75 mmol) were added to a stirred solution of 1-*O*-*tert*-butyl-4,5-*O*,*O*-diacetyl-(1*S*,3a*R*,4*R*,5*S*,7a*S*)-7a-methyl-octahydro-1*H*-indene-1,4,5-triol **9** in MeCN (20 mL), and the suspension was heated under reflux for 3 h. After cooling, the mixture was diluted with EtOAc (70 mL), and 10% aqueous Na_2SO_3 (20 mL) was added. The mixture was vigorously stirred until the iodine color disappeared. The organic layer was then separated and dried (Na_2SO_4). The solvent was evaporated, and the residue was filtered through a short silica gel column (EtOAc/hexane, 1:1) to give **10** (0.82 g, 97%): mp 65−67 °C (acetone−pentane−ether); $[\alpha]^{17}_D$ = −30.2 (*c* = 1.13); ν_{max} (KBr) 1745 cm^{-1} (C=O); ^{1}H NMR (400 MHz), δ (ppm) 1.01 (d, *J* = 0.6 Hz, 3H), 1.18−1.28 (m, 1H), 1.41−1.55 (m, 4H), 1.56−1.62 (br s, 1H), 1.69−1.77 (m, 1H), 1.80−1.97 (m, 2H), 1.99 (s, 3H), overlapping 2.05−2.18 (m, 1H), 2.12 (s, 3H), 3.59−3.65 (m, 1H, C), 4.77 - 4.84 (m, 1H), 5.36 (br d, *J* = 3.5 Hz, 1H); ^{13}C NMR (100 MHz), δ (ppm) 12.1, 20.99, 21.0, 21.1, 23.1, 30.2, 34.3, 42.0, 45.6, 70.4, 72.8, 80.6, 170.4, 170.7. Anal. Calcd for $C_{14}H_{22}O_5$ (270.32): C, 62.20; H, 8.20; found: C, 62.18; H, 8.19.

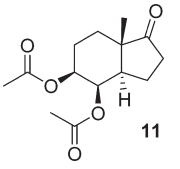

11

4,5-*O*,*O*-Diacetyl-(3a*R*,4*R*,5*S*,7a*S*)-4,5-dihydroxy-7a-methylo-octahydro-1*H*-inden-1-one (11). PCC (0.65 g, 3.00 mmol) was added at rt to a stirred solution of alcohol **10** (0.38 g, 1.41 mmol) in DCM (15 mL). After 1 h, the mixture was diluted with ether (15 mL) and filtered through a pad of Celite. The solvent was evaporated, and the residue was chromatographed on silica gel (39% EtOAc in hexanes) to give ketone **11** (a colorless oil, 0.34 g, 90%): $[\alpha]^{21}_D$ = +20.8 (*c* = 1.04); ν_{max} (film) 1742 cm^{-1}; ^{1}H NMR (400 MHz), δ (ppm) 1.13 (s, 3H), 1.35−1.47 (m, 1H), 1.70−1.95 (m, 5H), 1.99 (s, 3H) overlapping 2.10−2.20 (m, 2H), 2.12 (s, 3H), 2.43−2.52 (m, 1H), 4.80 - 4.89 (m, 1H), 5.50 (br d, *J* = 3.4 Hz, 1H); ^{13}C NMR (100 MHz), δ (ppm) 16.1, 20.3, 20.93, 20.98, 22.8, 29.4, 35.6, 45.9, 46.8, 70.7, 72.2, 170.2, 170.3, 218.0; MS HR (ESI) calcd for $C_{14}H_{20}O_5Na$ (MNa^+) 291.12030, found 291.12167.

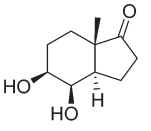

2

(3a*R*,4*R*,5*S*,7a*S*)-4,5-Dihydroxy-7a-methylperhydro-1-indenone (2). 10% aq NaOH (0.5 mL) was added to a solution of diacetate **11** (0.26 g, 0.98 mmol) in MeOH (10 mL). After 1 h, the mixture was filtered through a pad of silica gel, and the silica gel was washed with EtOAc. The solvent was evaporated to give diol **2** (0.18 g, 99%): $[\alpha]^{22}_D$ = +64.0 (*c* = 1.00); ν_{max} (film) cm^{-1} 3431, 1733 (C=O); ^{1}H NMR (400 MHz), δ (ppm): 1.15 (d, 3H, *J* = 3.4 Hz), 1.35−1.47 (m, 1H), 1.70−1.95 (m, 5H), 1.99 (s, 3H) overlapping 2.10−2.20 (m, 2H), 2.12 (s, 3H), 2.43−2.52 (m, 1H), 4.80 - 4.89 (m, 1H), 5.50 (br d, *J* = 3.4 Hz, 1H); ^{13}C NMR (100 MHz), δ (ppm) 16.1, 20.3, 20.93, 20.98, 22.8, 29.4, 35.6, 45.9, 46.8, 70.7, 72.2, 170.2, 170.3, 218.0; MS HR (EI) calcd for $C_{10}H_{16}O_3$ (M^+) 184.10994, found 184.11021.

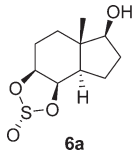

6a

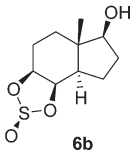

6b

(3a*S*,5a*S*,6*S*,8a*R*,8b*R*,2′*R*)-6-Hydroxy-5a-methyloctahydro-3a*H*-2λ-4-indeno[4,5-*d*][1,3,2]dioxathiolane 2-Oxide (6a) and (3a*S*,5a*S*,6*S*,8a*R*,8b*R*,2′*S*)-6-Hydroxy-5a-methyloctahydro-3a-*H*-2λ-4-indeno[4,5-*d*][1,3,2]dioxathiolane 2-Oxide (6b). Thionyl chloride (90 μL, 145 mg, 1.22 mmol) was added dropwise to a stirred at 0 °C solution of diol **2** (115 mg, 0.62 mmol) in DCM (3 mL) containing pyridine (223 μL, 219 mg, 2.76 mmol). After 15 min, the mixture was diluted with DCM (20 mL) and washed with water (15 mL), 10% aq tartaric acid (10 mL), and satd aq $NaHCO_3$ (10 mL). The organic solution was dried (Na_2SO_4), and the solvent was evaporated. The residue was dissolved in abs EtOH (5 mL) and cooled to 0 °C, and $NaBH_4$ (25 mg, 0.66 mmol) was added. The mixture was allowed to warm to rt (ca. 0.5 h), kept for an additional 0.5 h, and then diluted with EtOAc (30 mL). The solution was washed with water (20 mL) and brine (10 mL) and dried (Na_2SO_4). The solvent was evaporated, and residue was chromatographed on silica gel (20 g, 1% MeOH in DCM) to give a mixture of **6a** and **6b** (95 mg, 66%). A portion of this mixture (60 mg) was separated using preparative HPLC (Nucleosil 50/7 mm, two 250/2 mm columns connected in series, EtOAc/hexanes, 20:80) to give **6b** (colorless crystals, 17 mg, 28%) and **6a** (oil, 41 mg, 68%). **6b**: mp 139−141 °C; $[\alpha]^{24}_D$ = +2.4 (*c* = 0.38); ^{1}H NMR (400 MHz), δ (ppm) 1.06−1.17 (m, 1H) overlapping 1.14 (s, 3H), 1.48−1.73 (m, 5H), 1.86−2.00 (m 3H), 2.13−2.28 (m, 2H), 2.34−2.47 (m, 1H), 3.63 (ap.t, 1H, *J* = 8.6 Hz), 4.52- 4.62 (m, 2H); ^{13}C NMR

(100 MHz), δ (ppm) 11.0, 21.9, 27.0, 30.2, 33.9, 41.2, 44.8, 78.0, 80.6, 81.4; MS HR (ESI) calcd for $C_{10}H_{16}O_4NaS$ (MNa^+) 255.06615, found:255.06549. **6a**: $[\alpha]^{24}_D = -46.4$ ($c = 1.75$); ^{1}H NMR (400 MHz), δ (ppm) 0.96 (s, 3H), 1.09 (dt, $J = 17.4, 3.8$ Hz, 1H), 1.50−1.96 (m, 6H), 2.06−2.25 (m, 3H), 3.65 (ap t, 1H, $J = 8.6$ Hz), 4.77−4.85 (m, 1H), 5.08 (dd, $J = 5.0, 2.8$ Hz, 1H); ^{13}C NMR (100 MHz), δ (ppm) 11.6, 21.9 (CH_2), 26.2, 30.1, 33.0, 40.9, 43.6, 80.7, 80.9, 83.4; MS HR (ESI) calcd for $C_{10}H_{16}O_4NaS$ (MNa^+) 255.06615, found 255.06572.

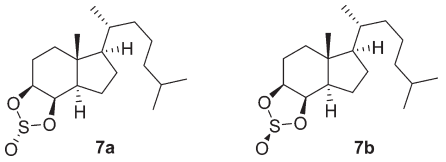

(3a*S*,5a*R*,6*R*,8a*R*,8b*R*,8*bR*,2′*R*)-6-[(1*R*)-1,5-Dimethylhexyl]-5a-methyloctahydro-3a*H*-2λ-4-indeno[4,5-*d*][1,3,2]dioxathiolane 2-Oxide (7a) and (3a*S*,5a*R*,6*R*,8a*R*,8b*R*,8*bR*,2′*S*)-6-[(1*R*)-1,5-Dimethylhexyl]-5a-methyloctahydro-3a*H*-2λ-4-indeno[4,5-*d*]-[1,3,2]dioxathiolane 2-Oxide (7b). Thionyl chloride (192 μL, 321 mg, 2.39 mmol) was added to a stirred at 0 °C solution of **3**[9] (381 mg, 1.35 mmol) in dichloromethane (6 mL) containing pyridine (480 μL, 465 mg, 5.93 mmol). After 15 min, the mixture was allowed to warm to room temperature, and the reaction was quenched by cautious addition of water (0.5 mL). Dichloromethane (20 mL) was then added, and the solution was washed with 5% hydrochloric acid and aqueous $NaHCO_3$, and dried (Na_2SO_4). The solvent was evaporated, and the residue was dissolved in dichloromethane (ca. 0.5 mL) and filtered through a short pad of silica gel. The crude product was chromatographed on silica gel (25 g, 1% EtOAc/hexane) to give **7b** (waxy solid, 120 mg, 27%) and **7a** (clear oil 323 mg, 73%). **7b**: mp 55−57 °C (MeOH); $[\alpha]^{20}_D = +22.3$ ($c = 1.00$); ν_{max} (film) 2954, 1212, 962 cm^{-1}; ^{1}H NMR (400 MHz) δ (ppm) 0.86 and 0.87 (2d, $J = 6.6$ Hz, 6H) 0.90 (d, $J = 6.4$ Hz, 3H), 0.95−1.22 (m, 4H) overlapping 1.05 (s, 3H), 1.25−1.82 (m, 8H), 1.86−2.02 (m, 1H), 2.04−2.18 (m, 3H), 2.34−2.46 (m, 1H), 2.34 (m, 1H), 4.57−4.61 (m, 1H); ^{13}C NMR (100 MHz), δ (ppm) 12.0, 18.5, 22.5, 22.7, 22.8, 23.8, 27.3, 27.8, 28.0, 35.1, 35.8, 36.7, 39.4, 41.0, 49.7, 55.8, 80.8, 83.9; MS HR (ESI) calcd for $C_{18}H_{32}O_3NaS$ (MNa^+) 351.19644, found 351.19673. **7a**: $[\alpha]^{30}_D = -18.6$ ($c = 1.00$); ν_{max} (film) 2955, 1209, 960 cm^{-1}; ^{1}H NMR (400 MHz), δ (ppm) 0.859 and 0.864 (2d, $J = 6.6$ Hz, 6H), 0.88 (s, 3H), 0.89 (d, $J = 5.7$ Hz, 3H), 0.95−1.21 (m, 6H), 1.25−1.81 (m, 9H), 1.90−2.05 (m, 3H), 4.75−4.82 (m, 1H), 5.08 (dd, 1H, $J = 5.1, 2.6$ Hz); ^{13}C NMR (100 MHz), δ (ppm) 12.5, 18.5, 22.5, 22.7, 22.8, 23.7, 24.4, 27.7, 28.0, 35.2, 35.7, 35.8, 39.4, 40.7, 48.5, 55.7, 78.3, 81.4; MS HR (ESI) calcd for $C_{18}H_{32}O_3NaS$ (MNa^+) 351.19644, found 351.19482.

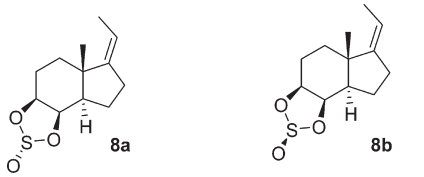

(3a*S*,5a*R*,6*R*,8a*R*,8b*R*,8*bR*,2′*R*)-6-[(1*R*)-1,5-Dimethylhexyl]-5a-methyloctahydro-3a*H*-2λ-4-indeno[4,5-*d*][1,3,2]dioxathiolane 2-Oxide (8a) and (3a*S*,5a*R*,6*R*,8a*R*,8b*R*,8*bR*,2′*S*)-6-[(1*R*)-1,5-Dimethylhexyl]-5a-methyloctahydro-3a*H*-2λ-4-indeno[4,5-*d*]-[1,3,2]dioxathiolane 2-Oxide (8b). The experiment was carried out as that described for **7b** using thionyl chloride (300 μL, 490 mg, 4.09 mmol), **4**[9] (417 mg, 2.12 mmol), dichloromethane (7.5 mL), pyridine (760 μL, 740 mg, 9.39 mmol), and then water (0.5 mL) and dichloromethane (25 mL). The crude product was chromatographed on silica gel (30 g, 3% EtOAc/hexane) to give **8b** (waxy solid, 89 mg, 17%) and **8a** (colorless crystals, 376 mg, 73%). **8b**: mp 50−55 °C; $[\alpha]^{23}_D = -60.7$ ($c = 1.01$); ^{1}H NMR (400 MHz) δ (ppm) 1.25 (s, 3H), 1.50−1.62 (m, 1H), 1.64 (dt, $J = 7.2, 2.0$ Hz, 3H), 1.68−1.95 (m, 3H), 2.20−2.57 (m, 5H), 4.53−4.60 (m, 1H), 4.64 (dd, $J = 5.3, 2.6$ Hz), 5.14 (qt, $J = 7.3, 2.0$ Hz, 1H); ^{13}C NMR (100 MHz), δ (ppm) 13.0, 17.4, 23.4, 27.5, 30.7, 34.2, 42.7, 55.8, 80.6, 83.7, 114.2, 147.3; MS HR (ESI) calcd for $C_{12}H_{18}O_3S$ (M^+) 242.09767, found 242.09873. **8a**: mp 104−105 °C (pentane); $[\alpha]^{25}_D = -46.3$ ($c = 1.10$); ^{1}H NMR (400 MHz) δ (ppm) 1.07 (s, 3H), 1.51−1.60 (m, 1H), 1.63 (dt, $J = 7.3, 2.0$ Hz, 3H), 1.66−1.77 (m, 4H), 2.09−2.17 (m, 1H), 2.24−2.35 (m, 2H), 2.47−2.55 (m, 1H), 4.79−4.86 (m, 1H,), 5.10 (m, 2H); ^{13}C NMR (100 MHz), δ (ppm) 13.0, 18.0, 23.4, 26.6, 30.7, 33.4, 42.3, 47.9, 78.1, 81.1, 114.4, 147.2. Anal. Calcd for $C_{12}H_{18}O_3S$ (242.34): C, 59.48; H, 7.49; S, 13.23. Found: C, 59.37; H, 7.37; S, 13.42.

Calculations. In our computations, all excited-state calculations have been performed using the Gaussian program package[15] and were based upon the ground-state geometries of single molecules. Rotatory strengths were calculated using both length and velocity representations. In the present study, the differences between the length and velocity of calculated values of rotatory strengths were quite small, and for this reason, only the velocity representations were taken into account (see also the Supporting Information). The CD spectra were simulated by overlapping Gaussian functions for each transition according to the procedure previously described.[16]

Conformational analyses were performed using CONFLEX[17] software and MM3 force field. Conformers found with the use of molecular mechanics were optimized using the B3LYP hybrid functional and small basis set 6-31 g(d). Then the conformers with relative energies ranging from 0 to 6 kcal mol^{-1} were reoptimized using the same hybrid functional and enhanced basis set 6-311++G(2d,2p). Finally, for these structures the frequency calculations were carried out at the B3LYP/6-311++G(2d,2p) level of theory to establish that the conformations are stable. For all compounds, the population percentages were calculated using both ΔE and ΔG values, applying Boltzmann statistics and $T = 298$ K. Due to their similarity only the ΔG values were considered further.

For all stable conformers found, the oscillator and rotatory strengths were calculated at the TD-B3LYP/6-311++G(2d,2p) and TD-B3LYP/6-311++G(2df,2p) theory levels. The calculated spectra were Boltzmann averaged according to the population percentages of individual conformers. The better fit to experimental spectra was obtained with the use of TD-B3LYP/6-311++G(2d,2p) method, so only these results were discussed. It should be noted that in the case of TD-B3LYP/6-311++G(2df,2p) method some artificial bands appeared. In the case of B3LYP/6-311++G(2d,2d) the calculated UV spectra were red-shifted by ca. 5−15 nm in relation to the experimental ones and were scaled by appropriate

(15) Frisch, M. J.; Trucks, G. W.; Schlegel, H. B.; Scuseria, G. E.; Robb, M. A.; Cheeseman, J. R.; Zakrzewski, V. G.; Montgomery, J. A. J.; Stratmann, R. E.; Burant, J. C.; Dapprich, S.; Millam, J. M.; Daniels, A. D.; Kudin, K. N.; Strain, M. C.; Farkas, O.; Tomasi, J.; Barone, V.; Cossi, M.; Cammi, R.; Mennucci, B.; Pomelli, C.; Adamo, C.; Clifford, S.; Ochterski, J.; Petersson, G. A.; Ayala, P. Y.; Cui, Q.; Morokuma, K.; Salvador, P.; Dannenberg, J. J.; Malick, D. K.; Rabuck, A. D.; Raghavachari, K.; Foresman, J. B.; Cioslowski, J.; Ortiz, J. V.; Baboul, A. G.; Stefanov, B. B.; Liu, G.; Liashenko, A.; Piskorz, P.; Komaromi, I.; Gomperts, R.; Martin, R. L.; Fox, D. J.; Keith, T.; Al-Laham, M. A.; Peng, C. Y.; Nanayakkara, A.; ChallacombeGonzalez, C.; Head-Gordon, M.; Replogle, E. S.; Pople, J. A. Gaussian, Inc.: Pittsburgh PA, 2003.

(16) Diedrich, C.; Grimme, S. *J. Phys. Chem. A* **2003**, *107*, 2524–2539.

(17) CaChe; WS Pro 5.0 ed.; Fujitsu Ltd.

factors: 0.930 for **5a**, 0.923 for **5b**, 0.952 for **6a**, 0.999 for **6b**, 0.930 for **7a**, 0.905 for **7b**, 0.970 for **8a** and 0.985 for **8b**. The calculated spectra for model compounds **12a** and **12b** were not wavelength corrected.

X-ray Analysis of Compound 5b. All measurements of crystal were performed using a KM4CCD κ-axis diffractometer with graphite-monochromated Mo Kα radiation. The crystal was positioned at 62 mm from the CCD camera. Total of 2400 frames were measured at 0.5° intervals with a counting time of 18 s. The data were corrected for Lorentz and polarization effects. Empirical correction for absorption was applied.[18] Data reduction and analysis were carried out with the Oxford Diffraction programs.[19]

The structure was solved by direct methods[20] and refined using SHELXL.[21] The refinement was based on F^2 for all reflections except those with very negative F^2. Weighted R factors wR and all goodness-of-fit S values are based on F^2. Conventional R factors are based on F with F set to zero for negative F^2. The $F_o^2 > 2\sigma(F_o^2)$ criterion was used only for calculating R factors and is not relevant to the choice of reflections for the refinement. The R factors based on F^2 are about twice as large as those based on F. All hydrogen atoms were located geometrically, and their positions and temperature factors were not refined. Scattering factors were taken from Tables 6.1.1.4 and 4.2.4.2 in ref 5.

(18) CrysAlis RED, O. D. L., version 1.171.28cycle2 β (release 25−10−2005 CrysAlis171 .NET) (compiled Oct 25 2005,08:50:05). Empirical absorption correction using spherical harmonics, implemented in SCALE3 ABSPACK scaling algorithm.

(19) CrysAlis CCD, O. D. L., Version 1.171.28cycle2 β; CrysAlis RED, Oxford Diffraction Ltd.,Version 1.171.28cycle2 β.

(20) Sheldrick, G. M. *Acta Crystallogr*. **1990**, *A46*, 467–473.

(21) Sheldrick, G. M. SHELXL93; University of Göttingen, Göttingen, Germany, 1993.

Acknowledgment. This work was supported by Grant Nos. N N204 056335 (M.K.) and N N204 238134 (J.W.) from the Ministry of Science and Higher Education. All calculations were performed at Poznań Supercomputing Center, Poland. The X-ray measurements were undertaken in the Crystallographic Unit of the Physical Chemistry Laboratory at the Chemistry Department of the University of Warsaw, Poland.

Supporting Information Available: General experimental methods, IR, ^{1}H and ^{13}C NMR, and MS spectra for reported compounds, X-ray crystallographic structures (ORTEP) of compound **5b** with respective CIF files and computational details. Calculated structures of boat conformers of **5a**−**8b** and model compounds *E*-**8a**, *E*-**8b**, **12a**, and **12b**; all calculated UV and CD spectra, total energies, relative energies, numbers of imaginary frequencies. and Cartesian coordinates for all optimized structures used in this work. This material is available free of charge via the Internet at http://pubs.acs.org.